Available online at www.sciencedirect.com
ScienceDirect
Journal of Crystal Growth 298 (2007) 198–201
JOURNAL OF CRYSTAL GROWTH
www.elsevier.com/locate/jcrysgro

GaN growth on 150-mm-diameter (1 1 1) Si substrates

Akinori Ubukata[a,b,*], Kazutada Ikenaga[a,b], Nakao Akutsu[a,b], Akira Yamaguchi[a,b], Koh Matsumoto[a,b], Toshiaki Yamazaki[a,b], Takashi Egawa[b]

[a]*Taiyo Nippon Sanso Corporation, 10 Ohkubo, Tsukuba 300-2611, Japan*
[b]*Nagoya Institute of Technology, Gokiso-cho, Showa-ku, Nagoya 466-8555, Japan*

Available online 29 November 2006

Abstract

Metalorganic chemical vapor deposition (MOCVD) of a crack-free, mirror surface of GaN on 150-mm-diameter (1 1 1) Si substrate was performed using a horizontal MOCVD system. We used the combination of an AlGaN/AlN nucleation layer with an AlN/GaN strained superlattice structure (SLS) for strain control. A good mirror surface morphology was obtained over the entire GaN surface. Transmission electron microscopy (TEM) showed that screw dislocations were terminated at the interface of the GaN top layer and SLS. A pit density of $4 \times 10^9\,cm^{-2}$ was determined by atomic force microscopy, the mean thickness of the GaN top layer was approximately 0.4 μm, and the uniformity (1 sigma) was 4.37%. Asymmetrical reciprocal-lattice space mapping (RSM) measurement and TEM observation showed that the GaN film was fully relaxed. Relaxation occurs at both the interface of the SLS and AlN buffer layer and the interface of the GaN top layer and SLS.

PACS: 81.05.Ea; 78.55.Cr

Keywords: A1. Substrates; A2. X-ray diffraction; A3. Metalorganic chemical vapor deposition; B1. Nitrides; B2. Semiconducting III–V materials

1. Introduction

There has been considerable interest in the growth of GaN on Si substrates because of its low cost, large size, good thermal conductivity and the potential for integration with Si-based devices [1–3]. Now, GaN growth on a larger-diameter Si substrate is being in demand.

To obtain high-quality GaN on Si substrates, a key technology is an interlayer structure between the GaN and the Si substrate. The only way to eliminate cracks is to control stress in the interlayer. Thus, for GaN growth on Si, strain engineering must first be considered. It has been reported that a low-temperature AlN interlayer is useful for a reduction in dislocation density from 10^{10} to $10^9\,cm^{-2}$. By a combination of an AlN interlayer, monolayer-thick SiN in situ masking and subsequent lateral overgrowth, a crack-free AlGaN/GaN transistor structure and a crack-free LED structure were demonstrated [1,2].

We have shown pit- and crack-free GaN on Si substrate with an AlGaN/AlN buffer grown at a temperature higher than 900 °C [3]. As a result, no cracks or pits were observed on the GaN surface for an AlGaN/AlN buffer of thickness greater than 40 nm. At the surface of the buffer layer, there were trapezoid-shaped AlN islands and coalescence occurred during the growth of GaN. It is thought that the AlGaN/AlN interlayer plays a role similar to a buffer layer, which is usually used for the growth of GaN on sapphire substrates [4].

The thermal mismatch between GaN and Si, which is opposite to that of GaN on sapphire, induces compressive stress in GaN on Si and results in cracking during cooling from the growth temperature. The sources of stress are general problems for the growth of thick GaN. An AlN/GaN strained superlattice structure (SLS), which is used for strain control [5,6] and for dislocation filtering, is also effective for reducing tensile stress and cracks in GaN on Si [7]. Ishikawa et al. [8] achieved crack-free GaN on

*Corresponding author. Taiyo Nippon Sanso Corporation, 10 Ohkubo, Tsukuba 300-2611, Japan.
E-mail address: Akinori.Ubukata@tn-sanso.co.jp (A. Ubukata).

0022-0248/$ - see front matter © 2006 Elsevier B.V. All rights reserved.
doi:10.1016/j.jcrysgro.2006.10.147

100-mm-diameter (1 1 1) Si substrate using a set of AlN/GaN SLs to manage strain. To date, high-quality InGaN LEDs on 100-mm-diameter Si substrates [9] and AlGaN/GaN HEMTs on 100- and 125-mm-diameter Si (1 1 1) substrates [6,7] have been reported.

To optimize the multilayer buffer structure over a large-diameter substrate, it is important to suppress the parasitic reaction between trimethylaluminium (TMA) and ammonia (NH_3). To this end, we have developed a laminar-flow gas injection reactor that can suppress the parasitic reaction even for the growth of AlGaN at atmospheric pressure over a 150-mm-diameter wafer plate [10]. In this study, GaN epitaxial layers were grown on 150-mm-diameter Si (1 1 1) substrates with multilayer buffer structures of AlN/GaN SLS on an AlGaN/AlN nucleation layer.

2. Experiments

In this study, GaN/Si samples were grown using a laminar-flow metalorganic chemical vapor deposition (MOCVD) reactor system (Taiyo Nippon Sanso Co., SR6000). The reactor has a 150-mm-diameter wafer platen susceptor and is designed to enable growth from low pressure to atmospheric pressure. The surface temperature was controlled within 1 °C over the entire wafer template region, confirmed by near-infrared irradiative temperature measurements. In these experiments, all layers were grown at the low-pressure growth of 45 kPa. Trimethylgallium (TMG), TMA and NH_3 were used as source gases of Ga, Al and N, respectively.

Before the growth of GaN on Si substrates, the Si substrates were etched in H_2SO_4 and then HF solution, and Si dangling bonds were terminated with hydrogen atoms. Before growth, the substrate was heated at 1150 °C for 10 min. The temperature was lowered to 1000 °C, and 40-nm-thick AlN buffer layers were grown, after which 50-nm-thick $Al_{0.26}Ga_{0.74}N$ intermediate layers were grown to cover the Si substrate completely. Subsequently, AlN/GaN SLSs were grown on the AlGaN layer at the same growth temperature. We fabricated the SLSs in a similar manner to the SLSs in our previous report [3]. The growth temperature was then raised to 1100 °C and a 400-nm-thick GaN film was grown.

High-resolution X-ray diffractometry (HRXRD) measurements were then conducted using a Spectris X'pert MRD diffractometer. TEM measurements were performed to obtain more detailed information on the defect structure by comparing the TEM results with the HRXRD results.

3. Results

First, the effects of growth temperature on the AlN buffer layer were investigated. For growth temperatures less than 1000 °C, the AlN grain pyramidal like in shape and increases in size with growth temperature. Using atomic force microscopy (AFM), the roughness R_a and peak-to-valley (*P–V*) value of AlN buffer layer were found to be 11.5 and 21 nm, respectively, at a growth temperature of 900 °C. In case of increase of growth temperature, R_a and *P–V* of AlN buffer layer became smaller, 1.52 and 11.8 nm, respectively, at a growth temperature of 1000 °C. The roughness R_a and *P–V* of AlN buffer layer at a growth temperature of 1100 °C became 0.82 and 6.6 nm, respectively.

For the growth of GaN/SLS at 1100 °C on AlN buffer layer, a mirror GaN surface was obtained with AlN grown less than 1000 °C. Three-dimensional island growth mode occurred for AlN grown at 1100 °C. In the following results, the AlN buffer layer was grown at 1000 °C.

Fig. 1 shows a GaN sample on 150-mm-diameter Si substrate. A mirror surface without cracks was obtained. In the figure, printed characters and words are reflected as a mirror image. A colored fringe pattern have a concentric-circle shape was observed. The roughness R_a and *P–V* were 0.0823 and 1.756 nm, respectively. From the thickness mapping data for GaN (not shown here), the standard deviation was found to be 0.037 μm, which corresponds to the obtained sigma value of 4.37%. Wafer bending in these samples showed spherical concave bowing, and the degree of wafer bowing was approximately 60 μm for the GaN layer thickness of 0.4 μm, which of the same order of magnitude as the result obtained by Sugahara et al. for 125-mm-diameter Si substrate.

Fig. 2 shows a cross-sectional bright-field TEM image. The period of the SLS was measured to be 24 nm (AlN: 4 nm; GaN: 20 nm). The TEM image shows that the (AlN/GaN) SLS has abrupt and smooth interfaces. We will now discuss the effect of the SLS on threading dislocations (TDs). Some types of TD were revealed by comparing TEM diffraction contrast analysis (shown in Fig. 2). High densities of both edge-type and screw-type dislocations were observed at the interface between the epitaxial layers and the Si substrate. There is a large stress owing to a large

Fig. 1. GaN sample on 150-mm-diameter Si substrate.

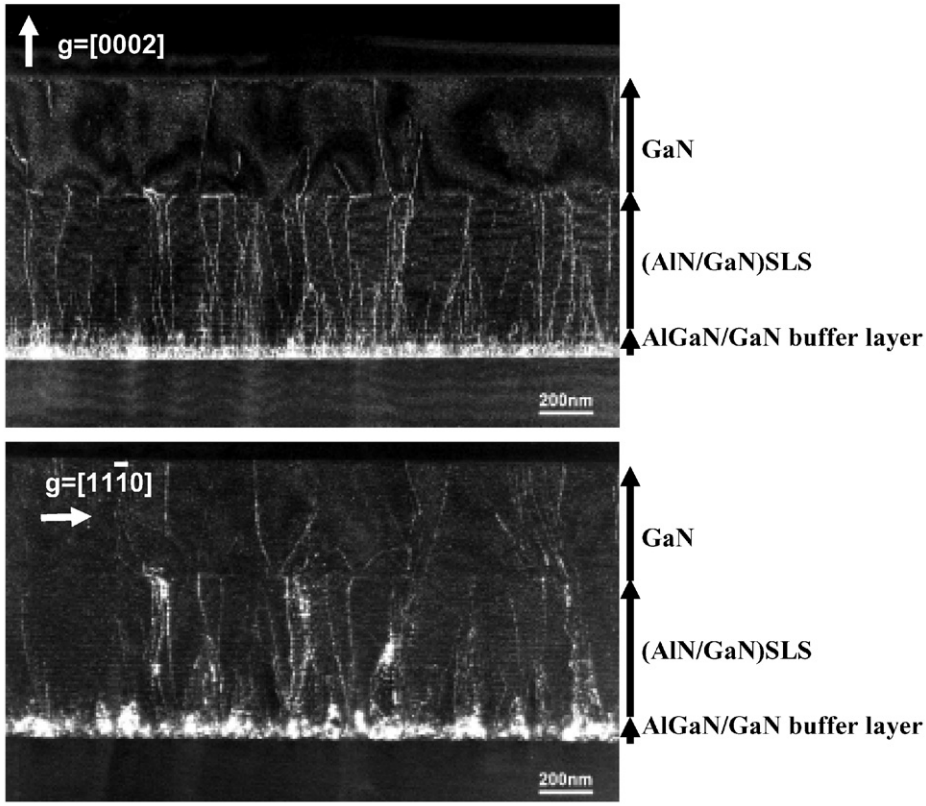

Fig. 2. Cross-sectional TEM image of GaN on Si.

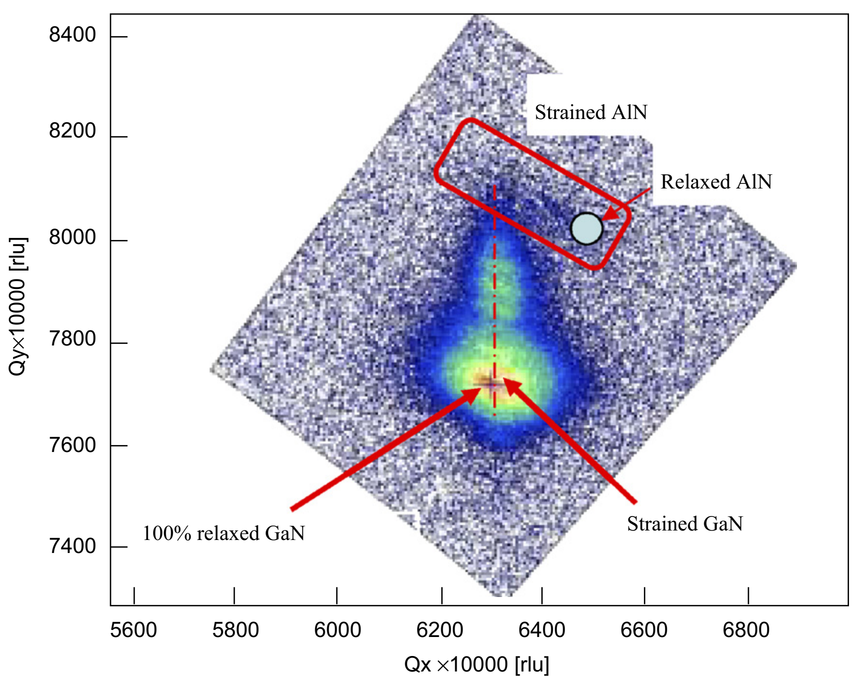

Fig. 3. RSMs for GaN on Si substrate.

lattice mismatch between AlN and Si. A plain AlN film on Si contains large dislocations due to strain relaxation of the film. In Fig. 2, the small-angle grain boundaries can be seen and three-dimensional growth mode was observed for AlN buffer layer. The strain relaxation occurs incompletely, and the strain is larger in the subsequently grown AlGaN or GaN than that on plain surface AlN. The AlN buffer layer induces a compressive stress in the subsequently grown

AlGaN or GaN layer partly counterbalancing both the growth-induced tensile stress and the thermally induced tensile stress during the cooling step [11].

Edge-type dislocations still remain in the GaN top layer with a Burgers vector of $g = [11\bar{1}0]$, and this indicates that SLSs have a negligible effect on blocking edge-type dislocations while screw-type dislocations are filtered in the SLSs and the interface of SLS and AlGaN. Wang et al. [12] concluded that (AlN/AlGaN) SLS was effective to eliminate dislocations while our results are different from those. AFM measurements show that the TD density at the surface is approximately $4 \times 10^9\,cm^{-2}$. An X-ray diffractometry rocking curve (XRD-RC) measurement with ω-scan was also performed on the 150 mm-diameter sample. The full-widths at half-maximum (FWHMs) of the (0 0 0 2) and $(1\,0\,\bar{1}\,2)$ XRD-RC were 980 and 1435 arcsec, respectively. In previous work, values of 650–740 arcsec for the (0 0 0 2) direction and 1500–1620 arcsec for the $(2\,0\,\bar{2}\,4)$ direction were obtained when the thickness of the AlN buffer layer was 8–500 nm.

Fig. 3 shows RSMs for GaN on Si substrate. In this sample, the AlN reciprocal-lattice points are distributed in the solid line box region in Fig. 3. Both completely relaxed and partly strained AlN phases exist in this region. It indicates relaxation occurs at the (AlGaN/AlN) buffer layer. In Fig. 3, the Q_x of GaN top layer and (GaN/AlN) SLS are 0.6273[rlu] and 0.6287[rlu], respectively. The value of Q_x for GaN top layer corresponds to fully relaxed GaN. This is important because the GaN layer minimal strain must be exerted on the top GaN layer to avoid cracking within the thickness and to allow doping appropriate for device growth [13]. It has been reported that the Si doping cause tensile stress in GaN films, although the substitution of Si for Ga only causes negligible changes in the lattice constant. Thus, Si-doped GaN is responsible for severer cracking with compensate the gross strain because AlN buffer layer induces a compressive stress in the subsequently grown AlGaN or GaN layer. This small change of Q_x value indicates that relaxation occurs at the interface between SLS and GaN top layer because Q_x value corresponds to a lattice constant. The growth interruption was introduced and the growth temperature was changed at the interface. It is supposed that small islands were started to form and the relaxation occurred at the interface. No relaxation was occurred in SLS because all fringe peaks have same Q_x.

4. Summary

In summary, crack-free GaN was grown on a 150-mm-diameter (1 1 1) Si substrate. A good smooth mirror surface was obtained. Asymmetrical RSMs and TEM observation showed that the GaN film was fully relaxed. Relaxation occurs at both the interface of the SLS and (AlGaN/AlN) buffer layer and the interface of the GaN top layer and SLS.

Acknowledgments

This work was partially supported by Special Coordination Funds for Promoting Science and Technology. The authors are grateful to Dr. K. Seo of SPECTRIS Corporation for the measurement of RSMs.

References

[1] J. Christen, O. Contreras, F. Bertram, T. Riemann, F.A. Ponce, A. Dadgar, A.J. Diez, A. Krost, in; Proceedings of the 11th International Conference MOVPE (ICMOVPE-XI) (2002) Thu-P2.
[2] A. Dadgar, M. Poschenriender, J. Blasing, O. Contreras, F. Bertram, T. Riemann, A. Rieher, M. Kunze, I. Daumiller, A. Krtschil, A. Diez, A. Kaluza, A. Modlich, M. Kamp, J. Christen, F.A. Ponce, E. Kohn, A. Krost, J. Crystal Growth 248 (2003) 556.
[3] H. Ishikawa, G.-Y. Zhao, N. Nakada, T. Egawa, T. Jimbo, M. Umeno, Jpn. J. Appl. Phys. 38 (1999) L492.
[4] K. Hiramatsu, S. Itoh, H. Amano, I. Akasaki, N. Kuwano, T. Shiraishi, K. Oki, J. Crystal Growth 115 (1991) 628.
[5] Y. Ishihara, J. Yamamoto, M. Kurimoto, T. Takano, T. Honda, H. Kawanishi, Jpn. J. Appl. Phys. 38 (1999) L1296.
[6] S. Sugahara, J.S. Lee, K. Ohtsuka, Jpn. J. Appl. Phys. 43 (2004) L1595.
[7] S. Arulkumaran, T. Egawa, S. Matsui, H. Ishikawa, Appl. Phys. Lett. 86 (2005) 3503.
[8] H. Ishikawa, M. Kato, T. Aoyama, S. Matsui, M. Hao, T. Egawa, T. Jimbo, The Institute of Electronics, Inform. and Commun. Engineers (IEICE), Technical Report ED2003-149, 2003.
[9] T. Egawa, T. Moku, H. Ishikawa, K. Ohtsuka, T. Jimbo, Jpn. J. Appl. Phys. 41 (2002) L663.
[10] H. Tokunaga, I. Waki, A. Yamaguchi, N. Akutsu, K. Matsumoto, J. Crystal Growth 189 (1998) 519.
[11] A. Reiher, J. Blasing, A. Dadgar, A. Diez, A. Krost, J. Crystal Growth 248 (2003) 563.
[12] H.-M. Wang, J.-P. Zhang, C.-Q. Chen, Q. Fareed, J.-W. Yang, M. Asif Khan, Appl. Phys. Lett. 81 (2002) 604.
[13] L.T. Romano, C.G. Van de Walle, J.W. Ager III, W. Gotz, R.S. Kern, J. Appl. Phys. 87 (2000) 7745.